

# MNDO-PM3 MO studies on the thermal isomerization of photochromic 1',3',3'-trimethyl-6-nitrospiro[2H-1-benzopyran-2,2'-indoline]

Yasuo Abe <sup>a,\*</sup>, Ren Nakao <sup>a</sup>, Toyokazu Horii <sup>a</sup>, Satoshi Okada <sup>a</sup>, Masahiro Irie <sup>b</sup>

<sup>a</sup> Research Institute for Advanced Science and Technology, Osaka Prefecture University, 1-2 Gakuen-cho, Sakai 593, Japan

<sup>b</sup> Institute of Advanced Material Study, Kyushu University, Kasugaoka-Koen 6-1, Kasuga, Fukuoka 816, Japan

Received 25 August 1995; accepted 13 October 1995

## Abstract

Semiempirical MNDO-PM3 quantum chemical calculations were carried out for the merocyanine-form isomers of 1',3',3'-trimethyl-6-nitrospiro[2H-1-benzopyran-2,2'-indoline] to reveal the thermal back reaction of the photochromic spiropyran. The thermal cyclization mechanism was discussed on the basis of the potential barrier heights during the conformational changes between the merocyanine-form isomers.

**Keywords:** 1',3',3'-Trimethyl-6-nitrospiro[2H-1-benzopyran-2,2'-indoline]; Thermal isomerization; MNDO-PM3 quantum chemical calculations

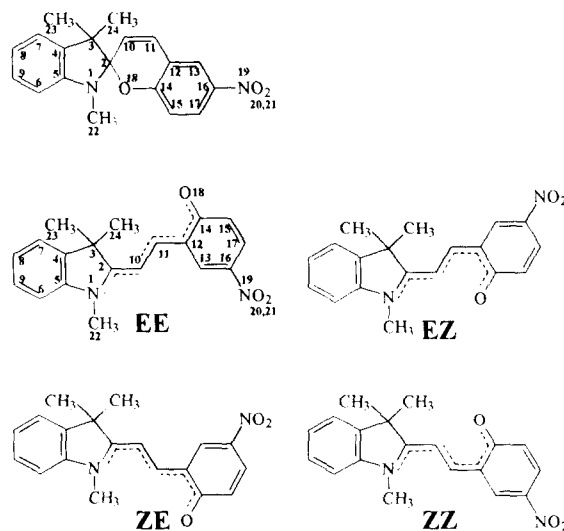
## 1. Introduction

1',3',3'-Trimethyl-6-nitrospiro[2H-1-benzopyran-2,2'-indoline] (**1**) is the most extensively studied photochromic compound [1]. UV irradiation of the colourless spiro isomer leads to cleavage of the C–O bond to give a coloured open-form isomer called photomerocyanine. The structures of the four pseudoplanar transoid stereoisomers of photomerocyanine and the spiro isomer are shown in Scheme 1. The cycloreversion of photomerocyanine to the colourless spiro isomer proceeds photochemically as well as thermally. Thermal cyclization takes place at room temperature, and the reaction kinetics have been extensively studied in various matrices [2–4]. In the present study, we have carried out semiempirical calculations on the reaction coordinate of the conformational changes between the merocyanine-form isomers to reveal the mechanism of the thermal back reaction of the spiropyran.

## 2. Computational method

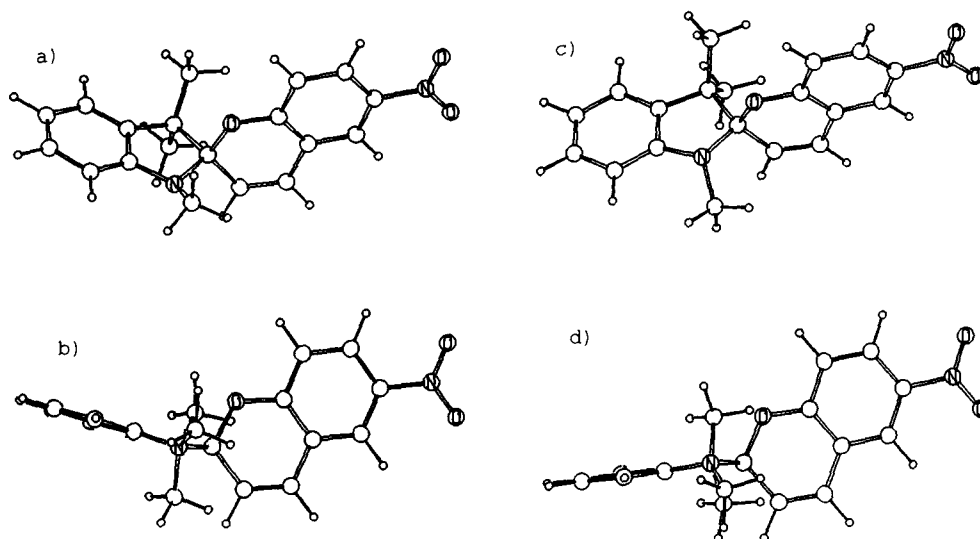
The calculations were carried out at the restricted Hartree–Fock (RHF) level with the MNDO-PM3 semiempirical SCF-MO method [5], as implemented in the MOPAC93 program

[6]. All geometrical variables for the stable isomers were fully optimized without making any assumptions, except for the carbon atom direction of the *N*-methyl group. The numbering of the atoms for the spiro- and merocyanine-form isomers is shown in Scheme 1. All stationary points were characterized by calculating the molecular vibrational frequencies. Transition states were determined by the reaction



Scheme 1.

\* Corresponding author.



Scheme 2.

coordinate method and verified by the existence of only one negative vibrational frequency.

### 3. Results and discussion

#### 3.1. Optimized structures and relative energies for the spiro- and merocyanine-form isomers

Optimization of the geometry of **1** led to two minima. Perspective views for the two conformers are shown in Scheme 2. One is a conformer (a) having an *N*-methyl group at the same side as the oxygen atom of pyran, as illustrated

in the side view (b). The other is a conformer (c) having an *N*-methyl group at the opposite side, as illustrated in the side view (d). Although the latter is  $0.54 \text{ kJ mol}^{-1}$  more stable than the former, conformer (c) was omitted from this discussion because X-ray crystallographic data of a bromo derivative have been reported to give the mirror image of conformer (a) [7].

The geometries for the merocyanine-form isomers were optimized by keeping the *N*-methyl group in the same direction in the spiro-form, i.e. the torsion angles  $C_{22}-N_1-C_2-C_3$  are negative. In the optimized structure for the merocyanine-form isomers, the indole ring and benzene ring are almost coplanar. The selected geometrical parameters, atomic

Table I  
Selected bond lengths (Å), torsion angles ( $^\circ$ ) and atomic charges of five isomers

	Closed	EE	EZ	ZE	ZZ	C=O group of acetone
<b>Bond lengths</b>						
C <sub>2</sub> -O <sub>18</sub>	1.442	5.119	3.981	5.186	3.960	
C <sub>14</sub> -O <sub>18</sub>	1.361	1.224	1.229	1.224	1.228	1.214
C <sub>2</sub> -C <sub>10</sub>	1.503	1.359	1.360	1.357	1.356	
C <sub>10</sub> -C <sub>11</sub>	1.337	1.429	1.421	1.428	1.424	
C <sub>11</sub> -C <sub>12</sub>	1.452	1.366	1.372	1.367	1.371	
<b>Torsion angles</b>						
C <sub>10</sub> -C <sub>2</sub> -C <sub>1</sub> -C <sub>3</sub>	-121.6	-177.7	-178.0	-175.9	-175.8	
C <sub>11</sub> -C <sub>10</sub> -C <sub>2</sub> -C <sub>3</sub>	114.6	-2.4	-2.5	-177.6	-177.1	
C <sub>12</sub> -C <sub>11</sub> -C <sub>10</sub> -C <sub>2</sub>	1.6	180.0	179.6	179.0	178.9	
O <sub>18</sub> -C <sub>2</sub> -C <sub>3</sub> -N <sub>1</sub>	-111.4	175.8	-179.8	171.4	176.8	
C <sub>22</sub> -C <sub>1</sub> -C <sub>2</sub> -C <sub>3</sub>	-157.8	-156.3	-158.9	-149.5	-147.4	
<b>Charge on N<sub>1</sub></b>						
Charge on C <sub>14</sub>	+0.002	+0.150	+0.164	+0.153	+0.141	
Charge on O <sub>18</sub>	+0.179	+0.362	+0.379	+0.361	+0.375	+0.250
Charge on N <sub>1</sub>	-0.185	-0.346	-0.363	-0.346	-0.352	-0.312
<b>H<sub>f</sub> (kJ mol<sup>-1</sup>)</b>						
Relative H <sub>f</sub>	73.07	105.12	114.33	109.34	119.94	
	-32.05	0.00	9.21	4.22	14.82	

charges and other physical properties are shown in Table 1. The bond lengths of  $C_{14}-O_{18}$  are slightly longer than the calculated bond length of  $C=O$  for acetone. The atomic charge on  $N_1$  is decreased by the scission of the  $C_2-O_{18}$  bond and that on  $O_{18}$  is increased. These results suggest that the merocyanine-form isomers have some zwitterionic character, which agrees with the experimental hypsochromic shift in polar solvents. All of the merocyanine-form isomers (four conformers) are less stable by as much as 32.03–46.85  $\text{kJ mol}^{-1}$  than the spiro-form isomer. Of the four conformers, the most stable is EE, the next ZE and the most unstable ZZ. (For the related molecule spironaphthoxazine, the most stable isomer has been reported as EZ, the next ZZ and the most unstable ZE by ab initio calculation [8].) The coloured form of some spiropyran has been reported to be the EZ isomer based on NMR measurements [9,10]. The energy profiles of

the isomerization processes are discussed below in order to clarify the above discrepancy.

### 3.2. Isomerization from EE to EZ

We start from the most stable EE conformer. The geometries for the reaction coordinate were calculated using a partial optimization technique by fixing the torsion angle  $C_{13}-C_{12}-C_{11}-C_{10}$  constant and keeping the torsion angle  $O_{18}-C_2-C_3-N_1$  negative. The potential energy curve for the isomerization from the EE to the EZ conformation is shown in Fig. 1(a). In the transition state (TS), the torsion angles  $C_{13}-C_{12}-C_{11}-C_{10}$  and  $O_{18}-C_2-C_3-N_1$  are  $91.70^\circ$  and  $-143.38^\circ$ . The heat of formation at the TS is 219.51  $\text{kJ mol}^{-1}$ . The barrier heights to the TS from EE and EZ are 114.39 and 105.25  $\text{kJ mol}^{-1}$  respectively. The  $EE \rightleftharpoons EZ$  process is allowed from both directions based on the potential energy calculation. The

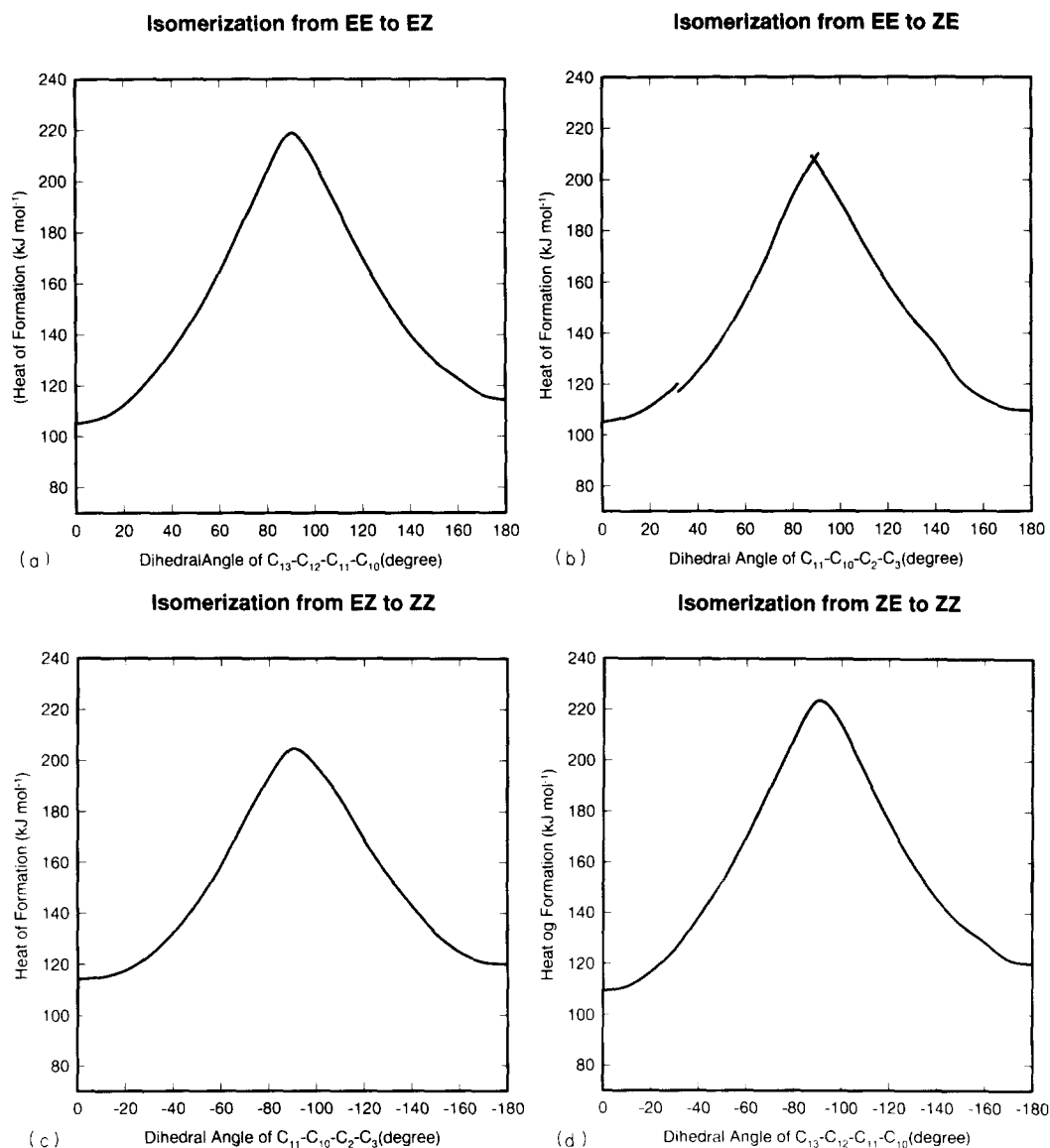


Fig. 1. Potential energy surfaces of thermal isomerization of photomerocyanine-form isomers: (a) from EE to EZ; (b) from EE to ZE; (c) from EZ to ZZ; (d) from ZE to ZZ.

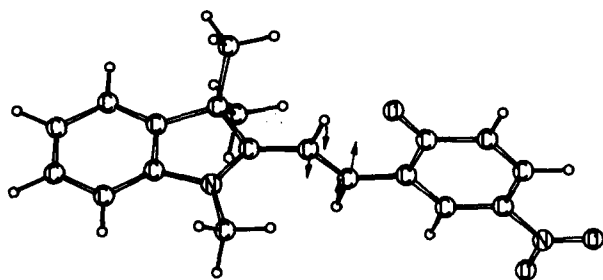


Fig. 2. Optimized structure at the TS for the isomerization from EZ to ZZ.

structure of the TS has a sole imaginary frequency of  $244.4\text{ cm}^{-1}$ . Isomerization by reverse rotation is impossible because the torsion angle  $C_{22}-N_1-C_2-C_3$  is discontinued in the reaction path.

### 3.3. Isomerization from EE to ZE

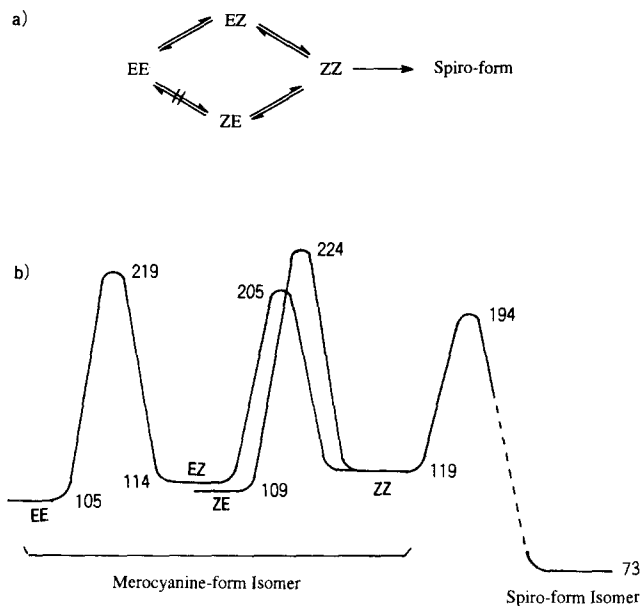
The geometries for the reaction coordinate were calculated by fixing the torsion angle  $C_{11}-C_{10}-C_2-C_3$  constant and keeping the torsion angle  $O_{18}-C_2-C_3-N_1$  negative. The potential energy curves for the isomerization from the EE to the ZE conformation are shown in Fig. 1(b). The TS was not found since the torsion angle  $O_{18}-C_2-C_3-N_1$  varies discontinuously from  $-141.1^\circ$  to  $-119.3^\circ$  when the torsion angle  $C_{11}-C_{10}-C_2-C_3$  is varied from  $90.46^\circ$  to  $90.47^\circ$ . This discontinuity involves the rotation of the phenyl ring and inversion of the *N*-methyl group. The result indicates that the  $EE \rightleftharpoons ZE$  process is prohibited. Reverse rotation also involves a similar discontinuity.

### 3.4. Isomerization from EZ to ZZ

The geometries for the reaction coordinate were calculated by the same procedure as for EE to ZE and the potential energy curve for the isomerization from the EZ to the ZZ conformation is shown in Fig. 1(c). In the TS, the torsion angles  $C_{11}-C_{10}-C_2-C_3$  and  $O_{18}-C_2-C_3-N_1$  are  $-91.24^\circ$  and  $-150.93^\circ$ . The heat of formation at the TS is  $205.05\text{ kJ mol}^{-1}$ . The barrier heights to the TS from EZ and ZE are  $90.79$  and  $85.11\text{ kJ mol}^{-1}$  respectively. The  $EZ \rightleftharpoons ZZ$  process is allowed from both directions. The structure of the TS shown in Fig. 2 has a sole imaginary frequency of  $174.7\text{ cm}^{-1}$ . The imaginary frequency vibrational mode is sketched. The modes correspond to the reaction path. The isomerization by reverse rotation is also possible and the barrier height of the TS is the same as for the former rotation.

### 3.5. Isomerization from ZE to ZZ

The potential energy curve for the isomerization from the ZE to the ZZ conformation, calculated by fixing the torsion angle  $C_{13}-C_{12}-C_{11}-C_{10}$  constant and keeping the torsion angle  $O_{18}-C_2-C_3-N_1$  negative, is shown in Fig. 1(d). In the TS, the torsion angles  $C_{13}-C_{12}-C_{11}-C_{10}$  and  $O_{18}-C_2-C_3-N_1$  are  $-91.77^\circ$  and  $-131.50^\circ$ . The heat of formation at the TS



Scheme 3.

is  $224.26\text{ kJ mol}^{-1}$ . The barrier heights to the TS from ZE and ZZ are  $114.93$  and  $104.32\text{ kJ mol}^{-1}$  respectively. The process  $ZE \rightleftharpoons ZZ$  is allowed from both directions. The TS has a sole imaginary frequency of  $261.1\text{ cm}^{-1}$ . Isomerization by reverse rotation is impossible because the torsion angle  $C_{22}-N_1-C_2-C_3$  is discontinued in the reaction path. The allowed and forbidden conformational changes between the four conformers are summarized in Scheme 3(a).

### 3.6. Cyclization of ZZ isomer

The geometries for the reaction coordinate were calculated by fixing the  $C_2-O_{18}$  bond length constant and keeping the torsion angle  $O_{18}-C_2-C_3-N_1$  negative, starting from the mirror image of the ZZ form shown in Table 1. A possible potential energy curve for the cyclization of the ZZ isomer to the spiro-form isomer is shown in Fig. 3(a). The energy maximum in the process was found at a bond length ( $C_2-O_{18}$ ) of  $2.116\text{ \AA}$ , a bond angle ( $O_{18}-C_2-C_3$ ) of  $106.0^\circ$  and a torsion angle ( $O_{18}-C_2-C_3-N_1$ ) of  $-94.3^\circ$ . The heat of formation at the TS is  $194.00\text{ kJ mol}^{-1}$ . The barrier height to the TS from ZZ is  $74.05\text{ kJ mol}^{-1}$ . The TS has a sole imaginary frequency of  $286.6\text{ cm}^{-1}$ . The spiro-form has the conformation (a) shown in Scheme 2. Although it requires various types of spin correlations, symmetry considerations and so on to judge whether or not real bond formation takes place, a smooth potential energy curve without a discontinuity is a necessary condition for cyclization to take place. Cyclization from the ZZ conformation satisfies the minimum requirement.

### 3.7. Cyclization of EZ, ZE and EE isomers

The geometries for the reaction coordinate from EZ, ZE and EE conformers to the spiro-form isomer were calculated by the same procedure as for the ZZ isomer. Potential energy

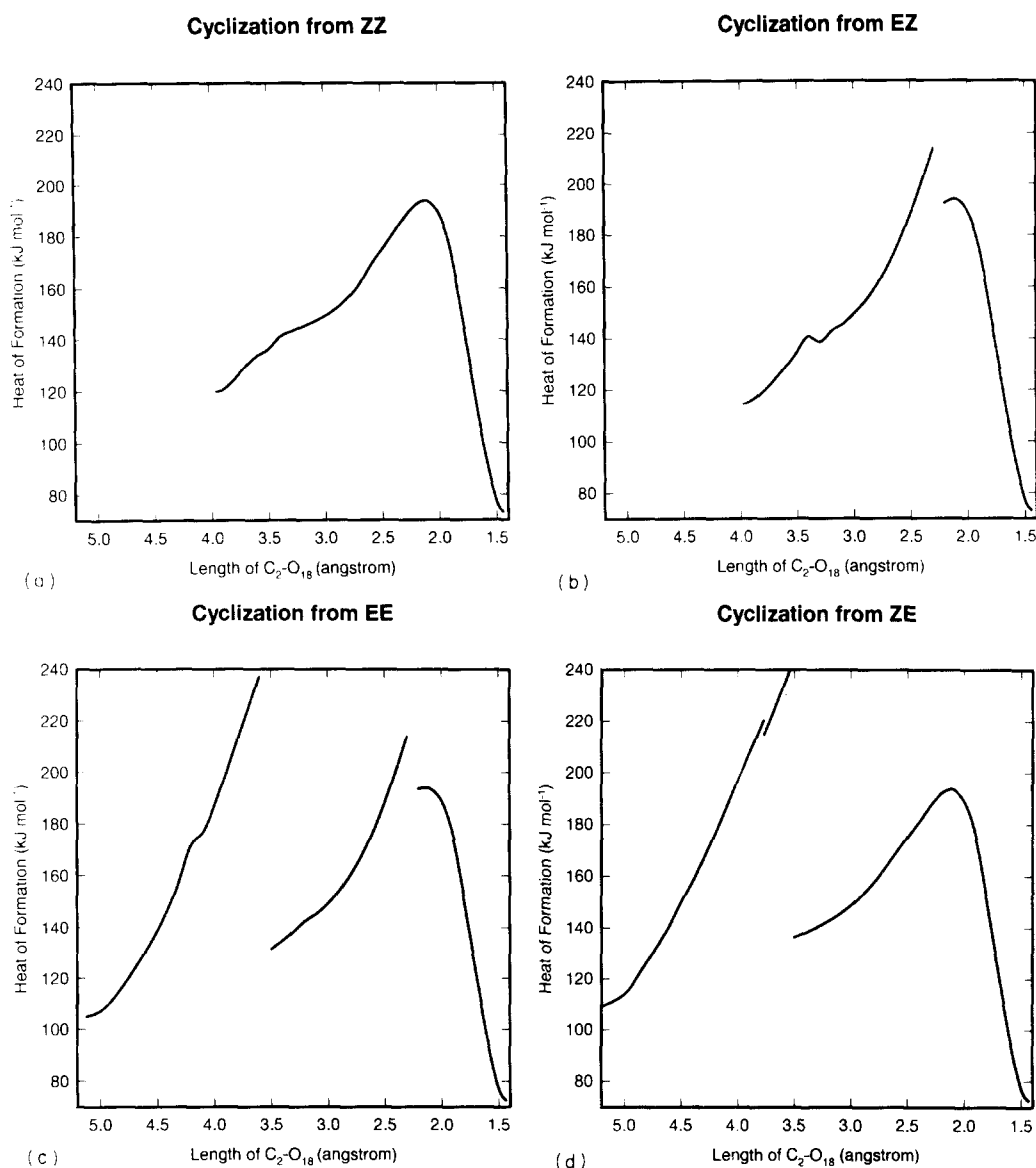


Fig. 3. Potential energy surfaces of thermal cyclization from photomerocyanine-form isomers: (a) from ZZ; (b) from EZ; (c) from EE; (d) from ZE.

curves for the cyclization of the three isomers are shown in Figs. 3(b)–3(d). In all cases, the potential energy curves show a discontinuity. The discontinuities indicate that direct single-step conversion from the EZ, ZE or EE conformers to the spiro-form isomer is prohibited. Careful examination of the potential energy curves reveals that the discontinuities are due to channel routes to other conformations, namely from EZ to ZZ and from ZE to ZZ. In the case of the EE conformer, two conformational changes from EE to EZ and EZ to ZZ are involved. The potential energy curve analysis supports the thermal cyclization processes shown in Scheme 3(a).

Of the four conformers of the merocyanine-form isomers, only the ZZ conformer was found to cyclize thermally through an appropriate reaction path. Isomerization from EZ to ZZ is necessary for the EZ form to cyclize to the spiro-form isomer. Two routes are possible for the isomerization

from EE to ZZ. One is via EZ and the other is via ZE. The route via ZE is prohibited as discussed in Section 3.3.

The fact that only the EZ form has been observed as a merocyanine-form isomer by NMR can be interpreted as follows. Although the EE conformer has the lowest energy, the large barrier from the EZ to the EE conformer suppresses population of the EE conformer. Therefore the EE conformer is not detected. The ZE conformer is more stable than the EZ conformer, but the population is less than that of the EZ conformer. This is due to the large barrier from the ZZ to the ZE conformer as shown in Scheme 3(b). The numbers denote the calculated heats of formation in  $\text{kJ mol}^{-1}$ . The photogenerated ZZ conformer mostly converts to the more stable EZ conformer and other conformers, ZE and EE, are not populated. This is the reason why the EZ conformer is the dominant merocyanine-form isomer. The thermal cyclization of

the EZ conformer is considered to proceed via the ZZ conformer.

### Acknowledgements

This work was partly supported by a Grant-in-Aid from the Tokyo Ohka Foundation for the Promotion of Science and Technology. The authors thank Professor A. Mizohata for the allotment of CPU time for EWS 4800/350 and the Computer Centre of the Institute for Molecular Science for that of SX-3/34R.

### References

- [1] H. Dürr, *Angew. Chem. Int. Ed. Engl.*, **28** (1989) 413.
- [2] R. Guglielmetti, in H. Dürr and H. Bouas-Laurent (eds.), *Photochromism: Molecules and Systems*, Elsevier, Amsterdam, 1990, pp. 323–330, and Refs. cited therein.
- [3] V. Krongauz, in H. Dürr and H. Bouas-Laurent (eds.), *Photochromism: Molecules and Systems*, Elsevier, Amsterdam, 1990, pp. 793–821.
- [4] R. Nakao, Y. Abe, T. Horii, T. Kitao and H. Inoue, *Nippon Kagaku Kaishi*, (1992) 1078.
- [5] J.J.P. Stewart, *J. Comput. Chem.*, **10** (1989) 209.
- [6] MOPAC93, Fujitsu Ltd.; J.J.P. Stewart, *Quant. Chem. Prog. Exch.*, **13** (1993) 40.
- [7] S.M. Aldoshin, L.O. Atovmyan, O.A. D'Yachenko and M.A. Gal' Bershtam, *Izv. Akad. Nauk SSSR, Ser. Khim.*, **12** (1981) 2720.
- [8] S. Nakamura, K. Uchida, A. Murakami and M. Irie, *J. Org. Chem.*, **58** (1993) 5543.
- [9] M. Inoue, M. Ueno and T. Kitao, *J. Am. Chem. Soc.*, **112** (1990) 8977.
- [10] S. Nakano, A. Miyashita and H. Nohira, *Chem. Lett.*, (1993) 13.